Inorganic Chemistry

Article

Cite This: Inorg. Chem. XXXX, XXX, XXX−XXX

pubs.acs.org/IC

Role of Seroalbumin in the Cytotoxicity of *cis*-Dichloro Pt(II) Complexes with (N^N)-Donor Ligands Bearing Functionalized Tails

Cristina Pérez-Arnaiz,[‡] Jorge Leal,[†] Natalia Busto,[‡] María C. Carrión,[†] Ana R. Rubio,[‡] Imanol Ortiz,[†] Giampaolo Barone,[§] Borja Díaz de Greñu,[†] Javier Santolaya,[‡] José M. Leal,[‡] Mónica Vaquero,[‡] Félix A. Jalón,[†] Blanca R. Manzano,[†] and Begoña García*[,‡]

[‡]Departamento de Química, Universidad de Burgos, Plaza Misael Bañuelos s/n, 09001 Burgos, Spain

[†]Facultad de Ciencias y Tecnologías Químicas-IRICA, Universidad de Castilla-La Mancha, Avda. Camilo J. Cela 10, 13071 Ciudad Real, Spain

[§]Dipartimento di Scienze e Tecnologie Biologiche, Chimiche e Farmaceutiche, Università degli Studi di Palermo, Viale delle Scienze Ed. 17, 90128 Palermo, Italy

Supporting Information

ABSTRACT: Given the potent anticancer properties of *cis*-diamminedichloroplatinum(II) and knowing its mode of action, we synthesized four new *cis*-[$PtCl_2$(N^N)] organoplatinum complexes, two with N-substituted pbi ligands (pbiR = 1-R-2-(2-pyridyl)benzimidazole) (namely, **1** and **2**) and two more with 4,4′-disubstituted bpy ligands (bpy = 2,2′-bipyridine) (namely, **3** and **4**). We explored their cytotoxicity and ability to bind to deoxyguanosine monophosphate (dGMP), DNA, and albumin models. By ^{1}H NMR and UV−vis spectroscopies, circular dichroism, agarose gel electrophoresis, differential scanning calorimetry measurements, and density functional theory calculations, we verified that only **3** can form aquacomplex species after dimethyl sulfoxide solvation; surprisingly, **1**, **2**, and **3** can bind covalently to DNA, whereas **4** can form a noncovalent complex. Interestingly, only complexes **1** and **4** exhibit good cytotoxicity against human ovarian carcinoma (HeLa) cell line, whereas **2** and **3** are inactive. Although lung carcinoma (A549) cells are more resistant to the four platinum complexes than HeLa cells, when the protein concentration in the extracellular media is lower, the cytotoxicity becomes substantially enhanced. By native electrophoresis of bovine seroalbumin (BSA) and inductively coupled plasma mass spectrometry uptake studies we bear out, on one hand, that **2** and **3** can interact strongly with BSA and its cellular uptake is negligible and, on the other hand, that **1** and **4** can interact with BSA only weakly, its cellular uptake being higher by several orders. These results point up the important role of the protein binding features on their biological activity and cellular uptake of *cis*-"$PtCl_2$" derivatives. Our results are valuable in the future rational design of new platinum complexes with improved biological properties, as they expose the importance not only of their DNA binding abilities but also of additional factors such as protein binding.

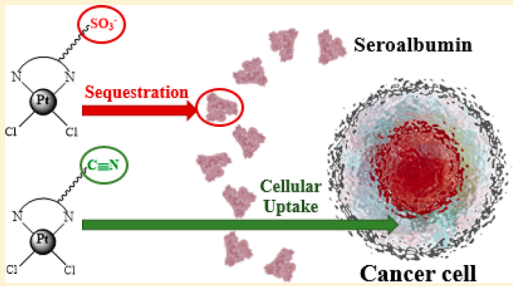

INTRODUCTION

Despite the notable advances in the discovery of new anticancer drugs that could become alternative to cisplatin, some of the disadvantages of this compound still remain satisfactorily unsolved so far.[1,2] It is therefore necessary to continue designing new active structural fragments and modify those that have proved to be ineffective, probably because they present limitations to reach their target. For example, factors such as protein binding and lipophilicity have a determinant impact on the absorption, distribution, metabolism, and excretion processes of the organic anticancer drugs.[3]

Thus, the favorable chemical formulation, size and shape, and the judicious inclusion of functional groups to achieve a favorable balance between lipophilicity and hydrophilicity are essential for the correct formulation of drugs. The presence of both lipophilic and hydrophilic groups in a drug can facilitate its administration and cell uptake. In the design of anticancer drugs, cellular uptake, lipophilicity, and cytotoxicity correlate in some instances.[4]

[$PtCl_2$(bpy)] (bpy = 2,2′-bipyridine) and other complexes with bpy bisubstituted in the 4,4′ positions and rollover cyclometalated Pt compounds based in the same backbone exhibit lower cytotoxic activity than cisplatin.[5,6] Comparable lack of marked activity has been found for the [$PtCl_2$(Hpbi)] (Hpbi = 2-(2′-pyridyl)benzimidazole) counterparts.[7,8] These results are surprising if one takes into account the notable cytotoxicity of many compounds with the *cis*-"$PtCl_2$" unit, and it might indicate the existence of limitations for these molecules to achieve their targets. By contrast, the organometallic derivate [PtMe(DMSO)(pbi)] (pbi = deprotonated form of Hpbi; DMSO = dimethyl sulfoxide), also neutral, shows a notable

Received: March 16, 2018

DOI: 10.1021/acs.inorgchem.8b00713
Inorg. Chem. XXXX, XXX, XXX−XXX

Chart 1. Synthesis of Ligands and Complexes 1−4 and Atom Numbering Scheme

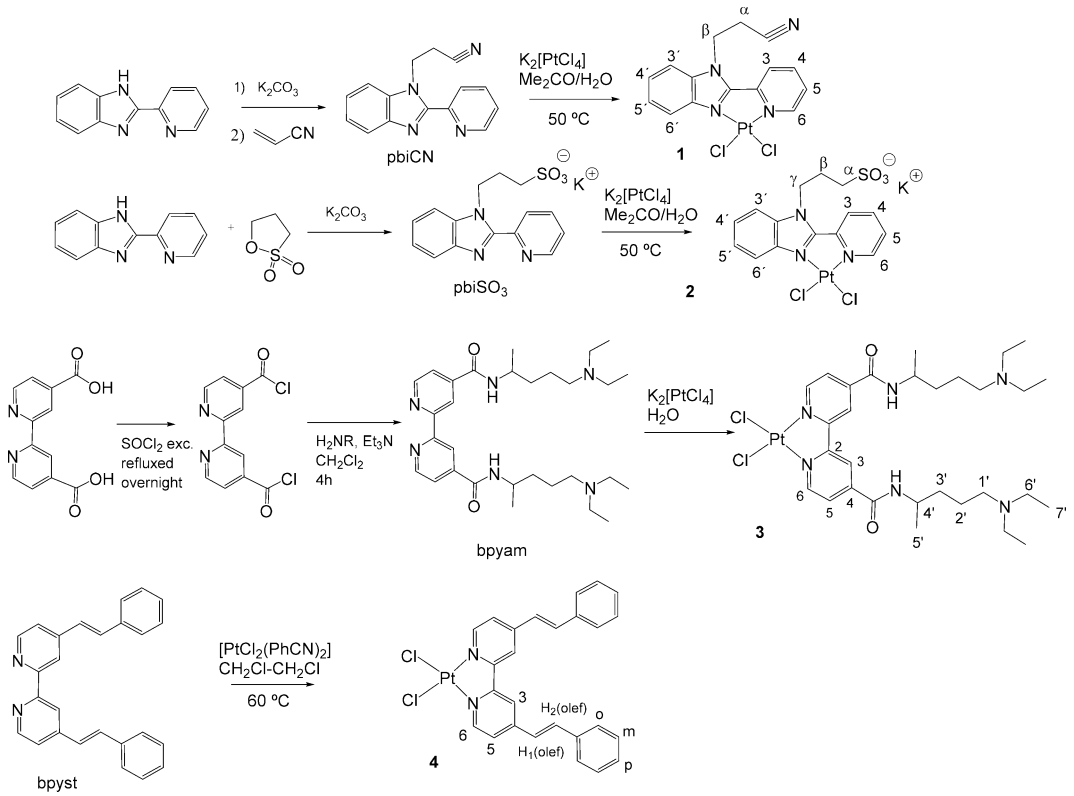

activity against A2780 and A2780R cancer lines,[9] indicating that minor changes can induce pronounced differences in the biological activity.

In this work, we propose introducing side lateral functionalized chains in both pbi and bpy ligands, synthesizing their *cis*-$PtCl_2$ derivatives and exploring their effect on the cytotoxicity and their ability to bind to DNA and protein models. With this in mind, the ligands and *cis*-$PtCl_2$ complexes included in Chart 1 were prepared. The side chains and functional groups were chosen considering bibliographic background in which these substituents exert a favorable action on the effect of different drugs. Thus, the cyano-ethyl fragment, present in complex **1**, had improved the cell permeability of drugs such as various Janus protein tyrosine kinases (JAK) inhibitors.[10] Alkylsulfonate groups, like that included in complex **2**, should become deprotonated in biological media if the low pK_a values for this functional group were considered, which could favor the solubility under physiological conditions. The biological activity of gold and silver N-heterocyclic carbenes bearing this group has been demonstrated both in bacteria[11] and in cancer cells.[12] The propylsulfonate chain forms part of merocyanine 540. This popular probe has been used as a model to study the permeation of cell membranes[13] and is an important active molecule, able to differentiate between the subtle differences in the plasma membranes of very similar cells such as leukemic and nonleukemic lymphocytes, depending on the composition of the culture medium.[14] The 5-diethylamino-2-pentylamino group, present in 4,4′-bis(*N*-(4-pentyldiethylamine)-carbamoyl)-2,2′-bipyridine (bpyam) ligand (see Chart 1) and in complex **3**, is a fragment widely used in drugs. Particularly relevant is its role in the formulation of the antimalarial drugs, chloroquine (CQ) and quinacrine (QC), where the stated aminated tail is responsible for the accumulation of the drug in the digestive vacuole of the pathogen, the site of the drug action.[15] Both of them are strong DNA intercalating agents with cytotoxic activity[16,17] that displays a synergistic effect in tumor cells treated with cisplatin.[18,19] In the case of the 4,4′-bis(*α*-styrene)-2,2′-bipyridine (bpyst)[20,21] ligand (Chart 1) the conjugation of the phenyl (Ph) ring and the ethylene fragment with the bpy unit renders this ligand very attractive due to its rigidity that enforces a plane structure.[22−24] Concerning our aims, the plane architecture makes [$PtCl_2$(bpyst)] (complex **4**) an interesting compound to be analyzed as a potential drug targeting DNA.

In this work, the synthesis, characterization and biological properties of these four new organocisplatin analogues are reported. Their binding properties to relevant biomolecules such as DNA and serum proteins and their cellular uptake are explored to establish which factors are determinant to their cytotoxicity, which could, in turn, lead to future rational structural modifications with improved biological activity.

RESULTS AND DISCUSSION

Synthesis and Structural Characterization. The complexes prepared in this work and their respective ligands are listed in Chart 1 along with their preparation methods. Even though the 1-(cyanoethyl)-2-(2-pyridyl)benzimidazole (pbiCN) ligand has been prepared previously,[25] the method described here is easier and provides a higher yield. This method consists of the deprotonation of the NH group of the commercially available 2-(2-pyridyl)benzimidazole and subsequent addition of acrylonitrile. The 1-(3-*n*-propylsulfonate)-2-(2-pyridyl)benzimidazole (pbiSO_3) and bpyam ligands are reported in this work for the first time. The pbiSO_3 ligand was prepared according to the procedure described for other *n*-propylsulfonate compounds,[26] by the reaction of 2-(2-pyridyl)-

DOI: 10.1021/acs.inorgchem.8b00713
Inorg. Chem. XXXX, XXX, XXX−XXX

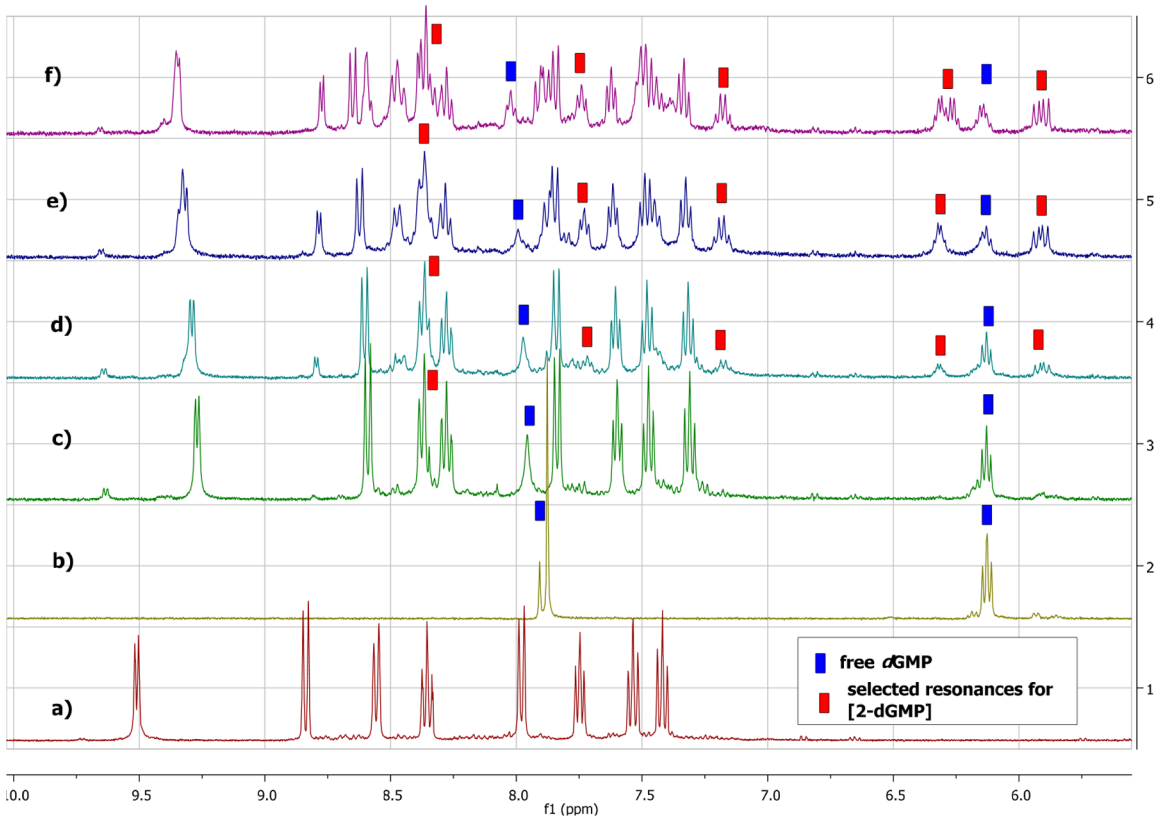

Figure 1. Aromatic area of ^{1}H NMR spectra in DMSO-d_6 of **2** + dGMP. (a) Complex **2** after 14 d in DMSO-d_6 + D_2O before addition of dGMP, (b) free dGMP, (c) t = 0, (d) t = 30 min, (e), t = 2 h, (f) t = 3 d.

benzimidazole in dimethylformamide (DMF) with 1,3-propane sultone in the presence of K_2CO_3 as deprotonating salt. The synthesis of the ligand bpyam was achieved by a classical amide formation procedure,[27] starting by the formation of the acid chloride of the 4,4′-dicarboxy-2,2′-bipyridine and ulterior reaction with the commercially available 5-diethylamino-2-pentylamine. Ligand 4,4′-bis(α-styrene)-2,2′-bipyridine (bpyst) was prepared as previously reported.[28]

Complexes **1**−**3** were prepared by the reaction of the $K_2[PtCl_4]$ salt with the respective ligands in water (**3**) or acetone/water (70:30 for **1** and 50:50 for **2**). While complex **3** was obtained at room temperature, the reaction to obtain **1** and **2** was performed at 50 °C. Complex **4** was obtained from the platinum precursor $[PtCl_2(PhCN)_2]$ from a 1,2-dichloroethane solution heated at 60 °C.

All the complexes were isolated in moderate-to-good yields (ranging from 54 to 74%) as yellow or orange-brown solids that were air and moisture stable. All of them are soluble in DMSO and relatively soluble in DMSO/H_2O mixtures, which facilitate the biological studies. The ligands and the complexes were characterized by ^{1}H, ^{13}C{^{1}H} NMR, and IR spectroscopies. Fast atom bombardment (FAB) mass spectra for the complexes were also recorded. The peaks observed are in accordance with the proposed formulations (see Experimental Section). The anionic complex **2** was characterized by FAB$^-$ spectrometry, showing the corresponding peak of the anion salt. In the IR spectra, the absorptions corresponding to the stretching vibrations of the C≡N,[29] SO_3^-,[30] (CO)NH, and C═C[31] functional groups were observed. The assignment of the NMR resonances was facilitated in some cases by two-dimensional experiments such as gCOSY, NOESY, gHSQC, and gHMBC. The NMR data with the corresponding assignments for the new ligands and for complexes **1**−**4** are shown in the Experimental Section. As expected, the coordination of the ligands causes deshielding in the ^{1}H NMR resonances of the protons of the coordinated rings. The effect is more marked (∼1 ppm) in the protons adjacent to the N-donor atoms and in $H^{6'}$ of **1** and **2** and H^3 of **3**. It is interesting to note the splitting of some proton (−C(O)N*H*, H^3) or carbon (CO, C^2, C^4, C^3, and $C^{4'}$) resonances of **3** as a consequence of the existence of two diastereomers, due to the presence of two chiral centers in the molecule. The weak base nature of the terminal −NEt_2 groups in **3** (pK_a = 12.8 in chloroquine) was evidenced in ^{1}H NMR spectrum in deuterated dimethyl sulfoxide (DMSO-d_6), since a very broad resonance around 9.5 ppm was present that disappeared as D_2O was added, as a consequence of deuterium exchange (Figure S3). The presence of this resonance was interpreted as evidence for protonation of this group by the residual water in the DMSO-d_6. As expected, the resonance assigned to the −C(O)N*H* group also exchanged with D_2O, and the corresponding signal was not observed in the spectrum.

Stability in DMSO and Aqueous Solution. The biological activity of cisplatin and its derivatives is known to be related to substitution of the chloride ligands by other solvent molecules such as H_2O, which then leads to covalent binding with DNA.[32] As the **1**−**4** complexes are very soluble in DMSO, the concentrated stock solutions (20 mM) were prepared in this solvent, and diluted solutions in aqueous buffer were then prepared prior to performing the biological experiments. Because of this, the stability of the complexes both in DMSO and in aqueous buffered solution was studied by

DOI: 10.1021/acs.inorgchem.8b00713
Inorg. Chem. XXXX, XXX, XXX−XXX

means of NMR, spectrophotometric measurements, and/or theoretical calculations.

Complex **1** is not soluble in DMSO/D_2O mixtures at the concentration required for the NMR experiments. Thus, the study of the substitution of the chloride ligand by DMSO and H_2O was studied by means of UV−vis spectroscopy, which allows working at much lower concentrations. As shown in Figure S1, after complex **1** dissolved in DMSO (10 μM) a two-exponential process takes place, pointing up the substitution of the two chloride ligands by DMSO molecules with rate constants of k_1 = 0.0017 s^{-1} (corresponding to formation of [PtCl(DMSO)(pbiCN)]Cl) starting from **1** and k_2 = 0.0002 s^{-1} (corresponding to formation of $[Pt(DMSO)_2(pbiCN)]Cl_2$). When water is added, the $[Pt(DMSO)_2(pbiCN)]Cl_2$ complex remains stable in solution, and no spectral changes with time are observed. Interestingly, ^{1}H NMR measurements show that, despite the similar structure of complexes **1** and **2**, the second is stable in solution and undergoes no substitution of the chloride ligands by DMSO-d_6 molecules in DMSO-d_6 solvent, neither by D_2O (see Figure S2). The ^{1}H NMR spectrum of the complex **3** in DMSO-d_6 shows a displacement with time of several resonances in the aromatic region of the spectrum, which indicates exchange of chloride ligands by one or two solvent molecules (see Figure S3.A). When deuterated water is added, aquation takes place, since a new complex appeared in solution after 10 h (Figure S3.B). The signals of complex **4** with time become broad both in DMSO-d_6 (Figure S4.A) and when deuterated water is added (Figure S4.B), making it difficult to obtain a reliable conclusion. To clarify this issue, UV−vis spectroscopy and density functional theory (DFT) calculations were also performed. The absorption spectra of **4** were recorded at different times after dissolution of the complex in DMSO (Figure S5.A). A monoexponential equation was fitted to the absorbance−time data pairs (Figure S5.B), indicating that the substitution occurs at least by one chloride ligand, the rate constant being k = 0.0005 s^{-1}. On the contrary, no kinetic effects are observed in solution when H_2O is added, indicating that aquation is absent. Indeed, DFT calculations reveal that the substitution of not only one but also two chloride units by DMSO molecules in **4** is thermodynamically favored through SN2 substitution (Figure S6.A), whereas the following substitution of DMSO by H_2O is not favored, as the hydrolysis product presents higher energy than the reactants (Figure S6.B). In details, both show higher values of the enthalpy versus the Gibbs free energy values for the transition states involved. The three self-consistent field (SCF) energy, enthalpy, and Gibbs free energy values point to same thermodynamic trend of the reaction pathway. In conclusion, from both the UV−vis experiments and DFT calculations, aquation for compound **4** can be discarded.

DNA Binding. As mentioned above, the biological activity of cisplatin analogues is usually related to formulation of covalent bonds with DNA. In particular, cisplatin is an inert compound that is activated by a series of aquation reactions in which one or both chloride ligands are substituted by H_2O molecules.[32] These mono- and biaquated cisplatin forms are highly reactive and prone to interact with different substrates, including DNA.[33] Because of this, the ability of **1**−**4** to bind to dGMP was first tested by means of ^{1}H NMR and $^{31}P\{^1H\}$ NMR studies. After addition of dGMP to a solution of complex **2**, ^{1}H NMR spectra showed the decrease of the intensity of the signals corresponding to free dGMP (see signal at 6.12 ppm) in the mixture, and new signals of the complex bound to the dGMP molecule were observed (see Figure 1). An incipient singlet at 8.35 ppm could be assigned to H8 of dGMP due to the binding of the platinum center to the N7 of the dGMP. The $^{31}P\{^1H\}$ spectra present a broad singlet centered at −1.5 ppm, and no more signals were observed in the spectra after time (see Figure S7). The nonobservation of resonances for lower fields conveys that O-coordination of dGMP is absent or is not significant. In the case of complex **3**, broadening of the ^{1}H NMR signals occurs after addition of dGMP, and an incipient singlet can be observed at 8.16 ppm after 2 d in solution, probably due to binding of the platinum center to N7 of dGMP (see Figure S8). This feature reveals that the covalent binding on **3** is rather slow compared to that of **2**.

Again, **1** could not be included in the NMR studies due to its insolubility in DMSO/D_2O mixtures at the required concentrations. Complex **4** also precipitated after addition of dGMP due to the relatively high concentrations needed.

To overcome this problem, circular dichroism (CD) experiments were performed in the presence of calf-thymus DNA (ctDNA). When complexes **1**−**4** were added to a ctDNA solution, **1**−**3** induced slow changes with time in the CD spectra, which stopped after 72 h, whereas the changes brought about by complex **4** were immediate. This observation excludes fast modes of binding like intercalation, which causes remarkable changes in the DNA structure in the microsecond time scale,[34] for complexes **1**−**3**. On the contrary, covalent binding to DNA is usually slower. Actually, the first signals related to formation of a covalent bond between **3** and dGMP appeared after 2 d of incubation. Thus, ctDNA was incubated with complexes **1**−**4** for 72 h to properly compare their ability to bind to DNA, thus distorting its structure in a longer time scale under the same experimental conditions. The CD spectra shown in Figure 2.A reveal pronounced structural changes in the DNA molecule upon binding of complexes **1**−**3**. As to complex **4**, as stated before, the NMR experiments with dGMP could not be performed, and the absence of changes in the CD spectra with time does not suffice to rule out covalent binding with DNA, as platinum complexes that can form monodentate covalent bonds do not significantly affect the CD spectra of DNA.[35] For that reason, agarose gel electrophoresis with pUC18 plasmid incubated with different contents of complex **4** (and also with cisplatin as a positive control for covalent binding) was performed. As shown in Figure S9, complex **4** does not induce changes in the migration of the characteristic plasmid DNA bands, whereas cisplatin provokes remarkable differences. This outcome allows one to exclude the presence of covalent binding between **4** and DNA. However, other modes of noncovalent interaction should not be ruled out. To assess such hypothesis, additional CD experiments were performed, and the relative elongation (L/L_0) was evaluated for different [complex]/[DNA] concentration (C_D/C_P) ratios. The CD spectra display an isoelliptic point at 250 nm, a slight lateral shift of the band centered at 275 nm, and a new induced CD band at 310 nm (Figure S10.A). This behavior, along with the changes in relative viscosity (Figure S10.B), is consistent with formation of a noncovalent complex between **4** and DNA.

Differential scanning calorimetry (DSC) experiments were performed to provide additional information about the binding features of complexes **1**−**4** to ctDNA. Figure 2.B shows the thermograms obtained at 25 °C for ctDNA incubated alone or in the presence of **1**−**4** at 0.5 C_D/C_P ratio for 72 h (higher concentration ratios could not be studied due to precipitation phenomena). In the case of complexes **1**, **2**, and **3**, for which

DOI: 10.1021/acs.inorgchem.8b00713
Inorg. Chem. XXXX, XXX, XXX−XXX

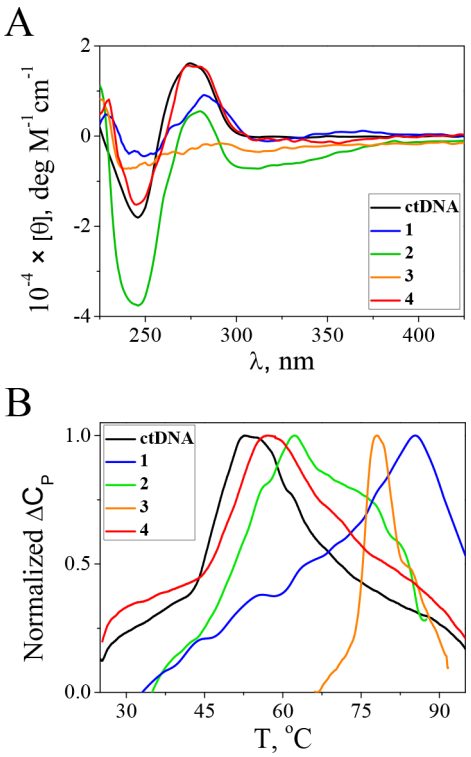

Figure 2. (A) CD spectra of ctDNA (P) incubated for 72 h with complexes **1**−**4** (D) at a concentration ratio $C_D/C_P = 1$ ($C_P = 8 \times 10^{-5}$ M) at T = 25 °C, C_{DMSO} = 0.4%. (B) DSC thermograms of ctDNA incubated for 72 h with complexes **1**−**4** at a concentration ratio $C_D/C_P = 0.5$ ($C_P = 4 \times 10^{-4}$ M) at a scan rate = 1 °C/min, C_{DMSO} = 1%. I = 2.5 mM sodium cacodylate (NaCac), pH = 7.4.

the covalent binding to dGMP has been confirmed previously by NMR experiments, the increases in T_m were 32.5, 9.7, and 25.3 °C, respectively. On the one hand, the largest ΔT_m values are induced by **1** and **3** and could be related to formation of interstrand cross-linking, which stabilizes the double-stranded DNA structure.[36] On the other hand, complex **4** induces a slight increase in T_m of 4.7 °C, which could be due to the presence of a noncovalent interaction between complex **4** and DNA, concurrent with the CD and viscosity observations.

The results obtained for the substitution of the chloride groups and for the covalent binding to dGMP and DNA for the four platinum complexes as well are summarized in Table 1. Interestingly, unlike cisplatin, clear correlation between the chloro substitution by DMSO and H_2O and the covalent binding with DNA for complexes **1**−**3** seems to be absent.

Table 1. Summary of the Results of the Substitution of the Chloride Ligands by DMSO and H_2O. Covalent Binding with DNA and Binding to BSA for the Complexes 1−4

complex	DMSO substitution	H_2O substitution	covalent binding to d GMP[a]	covalent binding to DNA	BSA binding[b]
1	√	×	n.o.	√	×
2	×	×	√	√	√
3	√	√	√	√	√
4	√	×	n.o.	×	×

[a]**1** and **4** could not be studied due to precipitation under the ^{1}H NMR experimental conditions. n.o., not observed. [b]For complex **4**, the interaction is only observed at high concentrations.

Only complex **3** can form the aqua complex, and, hence, it can bind to DNA by a similar mechanism as to cisplatin.

Cytotoxicity Studies. Once the binding ability of the four platinum complexes with DNA was assessed, their cytotoxic activity against human cervical carcinoma (HeLa) and human lung carcinoma (A549) cell lines was also evaluated by the 3-(4,5-dimethylthiazol-2-yl)-2,5-diphenyltetrazolium bromide (MTT) assay after 72 h of incubation time. For comparison purposes, the cytotoxicity of cisplatin was also tested. The half-maximal inhibitory concentration (IC_{50}) values are summarized in Table 2. Complexes **2** and **3** are essentially nontoxic, whereas

Table 2. Cytotoxic Activity of Complexes 1−4 and Cisplatin Expressed as IC_{50} Values (μM)

	IC_{50}, μM		
	HeLa[a]	A549[a]	A549[b]
1	15.4 ± 0.9	>100	39.7 ± 0.7
2	>100	>100	65 ± 3
3	>100	>100	>100
4	33 ± 2	>100	41.9 ± 0.9
cisplatin	14.0 ± 0.9[c]	17 ± 1	14 ± 1

[a]Serum-supplemented media (10% FBS). [b]Serum-deprived media (1% FBS). [c]Taken from ref 40.

1 is cytotoxic only toward HeLa cells. This is noteworthy, because all three complexes have been shown to bind covalently to DNA. As to complex **4**, it can interact noncovalently with DNA and presents intermediate cytotoxicity toward HeLa cells. Note that **3** displays no cytotoxicity, even though it can form the aquacomplex and interact by covalent binding with DNA, a behavior similar to that of cisplatin; that is, the type of the DNA interaction is not the determining factor in the cytotoxicity of these *cis*-$PtCl_2$ derivatives. This set of results raises the question of which factors, such as cellular uptake or protein binding, could play a key role in their cytotoxicity.[4]

Many new metal complexes with novel modes of action have been reported, and their anticancer activity was linked to selective protein interaction that may lead to improved accumulation in the tumor, higher selectivity, and/or enhanced antiproliferative efficacy.[37] However, it was reported previously that the binding of metal complexes to certain proteins present in the cell culture media can affect negatively their uptake due to protein sequestration of the drug, thus affecting their biological activity.[3,38] To shed some light into this issue, the cytotoxic activity of the complexes was tested against A549 cells in a comparative manner, using not only standard serum supplemented (10% fetal bovine serum (FBS)) but also a serum-deprived (1% FBS) cell culture media. FBS contains a large amount of proteins that can interact strongly with certain drugs, which can in turn decrease drastically their bioavailability. Indeed, the cytotoxicity of complexes **1**, **2**, and **4** increased notably in serum-deprived media (see Table 2), in which the protein concentration is much lower. Cisplatin is known to interact very weakly with human serum albumin (HSA; $K = 8.52 \times 10^2$ M^{-1}),[39] which explains why its cytotoxicity is nearly the same in the presence of 10% or 1% FBS. Taking into account this set of results, it seems clear that the interaction with serum albumin present in the culture medium plays a critical role in the antiproliferative activity of cisplatin derivatives. This behavior has been observed recently in organic complexes[3] and gold derivatives.[33]

DOI: 10.1021/acs.inorgchem.8b00713
Inorg. Chem. XXXX, XXX, XXX−XXX

Protein Binding. Serum albumin plays a key role in drug delivery due to its binding properties and abundance in blood plasma. Bovine serum albumin (BSA) is a suitable model for protein binding because of its resemblance to HSA.[41] Therefore, in view of the effect of the FBS concentration in the cytotoxicity of platinum complexes, native acrylamide electrophoresis experiments of BSA were performed to further examine whether the protein binding could be determinant as to their cytotoxic activity. BSA was incubated for 72 h with complexes **1**–**4** in the dark at 25 °C for C_D/C_P concentration ratios of 10 and 20, and then native acrylamide electrophoresis was performed (Figure 3). Lanes 1 and 2 correspond to BSA

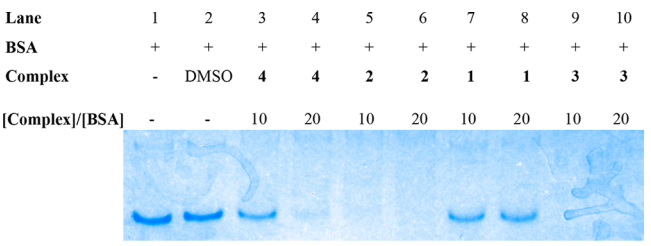

Figure 3. Native acrylamide electrophoresis of BSA incubated with complexes **1**–**4** for 72 h for [complex]/[BSA] concentrations ratios of 10 and 20. C_{BSA} = 1.5 μM, C_{DMSO} = 0.3%.

alone and in the presence of the maximum DMSO concentration used in the experiment (0.3%). Noteworthy, complexes **2** and **3**, which can interact with DNA through covalent bonding but display poor cytotoxicity, affect in a deep manner the protein conformation (lanes 5–6 and 9–10). Complex **4** also interacts with BSA, but higher concentrations are needed to affect the BSA conformation, as there is still no noticeable effect on the protein conformation at C_D/C_P = 10 (lane 3). On the contrary, complex **1**, the most cytotoxic, does not affect the BSA conformation even at high C_D/C_P ratios (lanes 7–8).

As shown in Figure 4, circular dichroism experiments confirmed the native electrophoresis results. The incubation

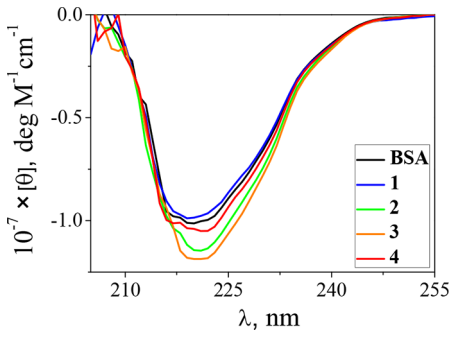

Figure 4. CD spectra of BSA in the absence and in the presence of the four platinum complexes **1**–**4** at a [complex]/[BSA] concentration ratio of 5. C_{BSA} = 0.5 μM, C_{DMSO} = 0.002%, I = 2.5 mM sodium cacodylate (NaCac), pH = 7.4, and T = 25 °C.

of BSA with complexes **2** and **3** induced a marked change in its characteristic λ = 220 nm negative band. Complex **4** also modified slightly this band, whereas complex **1** had almost no effect on the shape and intensity of the protein band.

As, on one hand **1** and **2** and on the other hand **3** and **4** differ only in their tails, we can conclude that the tail plays a determining role in their interaction with the protein. Very recently it has been reported that chloroquine (the lateral chain located on the backbone of complex **3**) can bind to HSA.[42] At pH = 7, chloroquine (CQ) is doubly protonated in both the N pyridine and ethylamine sites, as the resulting pK_a values are 8.4 and 10.8, respectively.[43] From comparison of CQ with complex **3**, we can state that in aqueous solution at pH = 7 the two ethylenamine groups are protonated (see ^{1}H NMR in Figure S3A). In this sense, MS-FABS$^+$ shows that, in 15% DMSO, complex **3** is in the $[M^+2H]^+$ form; therefore, in 0.3% DMSO (the solvent utilized to study the interaction with BSA) the two amines of the lateral chains will be fully protonated. Thus, the positive charge favors the electrostatic interaction with the negative net charge of the protein. Likewise, it was found that negatively charged compounds bind to HSA more strongly than expected from the lypophylicity of the ionized species at pH 7.4,[44] which is the case of complex **2**. Moreover, it has been observed that the binding of Merocyanine 540 to erythroid cells is hindered by the presence of serum proteins in the media,[14] probably due to the presence of a propylsulfonate chain in its structure. Thus, this moiety is determining for the interaction of complex **2** with BSA. In summary, the sets of observations point to a key role of protein binding in the cytotoxic properties of the platinum complexes, insofar as it could prevent the complexes from entering the cell. The binding to BSA clearly depends on the structure and charge of side lateral functionalized chains, the neutral chain remaining essentially noninteracting. For this reason, the cellular uptake of each complex was studied by inductively coupled plasma mass spectrometry (ICP-MS).

Cellular Uptake. The ability of the platinum complexes **1**–**4** to enter the cell was also studied to compare their uptake rates with their protein binding properties. Cells were incubated for 24 h with 10 μM of each complex, and then the amount of Pt in one million cells was measured by ICP-MS. In excellent agreement with the native protein electrophoresis and CD results, complexes **1** and **4**, which display weak affinity to BSA, are capable of entering the cell, showing high accumulation rates (Figure 5). On the contrary, complexes **2**

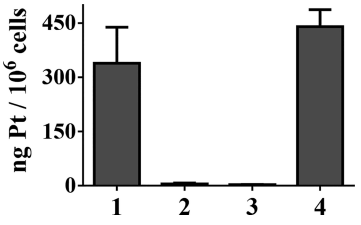

Figure 5. Metal accumulation in A549 cells after 24 h of exposure to 10 μM of complexes **1**–**4** expressed as microgram of Pt in one million cells.

and **3** were unable to enter the cell, probably due to protein sequestration in the media, which also explains their poor cytotoxicity in all cell lines.

CONCLUSIONS

Four new platinum(II) analogue complexes (**1**–**4**) to cisplatin have been synthesized and characterized, and their biological properties have been studied. Investigations on new antitumor Pt complexes have been focused since several decades ago on finding similar behaviors to that of cisplatin. Interestingly, we have verified that aquation is not a necessary step to bind covalently to DNA. Moreover, although albumin proteins have

DOI: 10.1021/acs.inorgchem.8b00713
Inorg. Chem. XXXX, XXX, XXX–XXX

been largely regarded as potential anticancer targets, we have shown that the interaction with BSA correlates with poor cell uptake of the platinum complexes, as occurs with complexes **2** and **3**, which can interact covalently with DNA but are prevented from reaching their target because of this strong interaction. By contrast, complexes **1** and **4**, which interact with DNA by covalent and noncovalent binding, respectively, are more cytotoxic, because they display weak effect on BSA, and, consequently, accumulation of the metal complex in tumor cells increases, improving their antiproliferative efficacy. In view that **1** and **2**, on one hand, and **3** and **4**, on the other hand, differ only by the lateral chain located on the same structural backbone, we can conclude that the nature of these chains is key to their remarkably different behavior. In conclusion, although the anticancer activity of *cis*-$PtCl_2$ derivatives has been linked to DNA interaction through covalent binding, we have demonstrated that their antiproliferative capacity can be diminished due to sequestration of the complexes by serum albumin, which could be useful in the future design of more potent platinum derivatives.

EXPERIMENTAL SECTION

Physical Methods. All synthetic manipulations were performed under an inert, oxygen-free, dry nitrogen atmosphere using standard Schlenk techniques. Solvents were distilled from the appropriate drying agents and degassed before use. Elemental analyses were performed with a Thermo Quest FlashEA 1112 microanalyser. The analytical data for the new complexes were obtained from crystalline samples where possible. IR spectra were recorded on a Shimadzu IR Prestige-21 IR spectrophotometer equipped with a Pike Technologies ATR. Only relevant bands are collected. FAB MS (position of the peaks in Da) were recorded with an Autospec spectrometer or a Thermo MAT95XP mass spectrometer with a magnetic sector. NMR spectra were recorded at 298 K on a Varian Unity Inova 400 or on a Varian Innova 500 spectrometer. ^{1}H and ^{13}C{^{1}H} NMR chemical shifts were internally referenced to tetramethylsilane (TMS) via the residual ^{1}H and ^{13}C signals of $CDCl_3$ (δ = 7.26 ppm and δ = 77.16 ppm), DMSO-d_6 (δ = 2.50 ppm and δ = 39.52 ppm), and D_2O (δ = 4.79 ppm) according to the values reported by Fulmer et al.[45] Chemical shift values are reported in parts per million, and coupling constants (J) are in hertz. The splitting of proton resonances is defined as s = singlet, d = doublet, t = triplet, q = quadruplet, m = multiplet, bs = broad singlet. 2D NMR spectra were recorded using standard pulse−pulse sequences: COrrelation SpectroscopY (COSY), Nuclear Overhauser Enhancement SpectroscopY (NOESY), Heteronuclear Multiple Quantum Coherence (HMQC), Heteronuclear Multiple Bond Correlation (HMBC). The probe temperature (±1 K) was controlled by a standard unit calibrated with a methanol reference. All NMR data processing was performed using MestReNova version 6.1.1.

Materials. Unless otherwise stated, reagents and solvents used were commercially available reagent quality. Conventional solvents and K_2CO_3 were purchased from Scharlab. Deuterated solvents were purchased from Eurisotop. $K_2[PtCl_4]$ was purchased from Johnson Matthey PLC. $[PtCl_2(PhCN)_2]$[46] and the ligands pbiCN[25] and bpyst[28] were prepared according to the literature. 4,4′-dicarboxy-2,2′-bipyridine, 4,4′-dimethy-2,2′-bipyridine, 2-(2-pyridyl)benzimidazole, acrylonitrile, 1,3-propanesultone, $SOCl_2$, 2-amine-5-diethylaminopentane, and trimethylamine were purchased from Across Organics.

The synthesized Pt(II) complexes can be referred to as dyes/drugs, and their molar concentration is expressed as C_D. Calf thymus DNA (lyophilized sodium salt, highly polymerized) from Sigma-Aldrich was dissolved in water and sonicated, producing short polynucleotide fragments (ca. 1000 base pairs). The molar DNA concentration is expressed in base pairs, ε (260 nm) = 13 200 M^{-1} cm^{-1}.[47] BSA was supplied by Sigma-Aldrich as crystallized and lyophilized powder (≥98%, agarose gel electrophoresis and ≤0.005% fatty acids); its concentration was spectrophotometricaly determined at 278 nm using absorptivity (ε) of 45 000 M^{-1} cm^{-1}.[48] Plasmid pUC18 (2686 bp) was extracted from *Escherichia coli* DH5α and purified by a HP Plasmid Midi kit (Omega Biotek, VWR). The concentrations of the polymers (ctDNA, BSA, and pUC18) are denoted as C_P.

Synthesis of Ligands and Complexes. *1-(Cyanoethyl)-2-(2-pyridyl)benzimidazole (pbiCN).* K_2CO_3 (318.6 mg, 2.3 mmol) was added to a solution of 2-(2-pyridyl)benzimidazole (300 mg, 1.5 mmol) in DMF (3 mL). The mixture was stirred at room temperature for 30 min. Then, 101 μL of acrylonitrile (1.5 mmol) was added, and the reaction was stirred for 4 h. The solvent was removed by vacuum evaporation resulting in a beige solid that was extracted with 10 × 3 mL of $CHCl_3$. The organic extracts were combined, obtaining 289.2 mg of the pure product, beige colored, after drying under vacuum. Yield, 76%.

3-(2-(2-pyridyl)-benzimidazol-1-yl)propane-1-sulfonate (pbiSO$_3$). A solution containing 318.6 mg of K_2CO_3 (2.3 mmol) was added over another with 2-(2-pyridyl)benzimidazole (300 mg, 1.5 mmol) in DMF (3 mL). The mixture was stirred at room temperature for 30 min. Then, 135 μL of 1,3-propanesultone (1.5 mmol) was added, and the mixture was stirred for 24 h. The mixture was filtered, and the solvent was removed by evaporation under vacuum. A yellow solid was obtained. 265.3 mg, yield: 55%. ^{1}H NMR (DMSO-d_6, 298 K): 8.79 (d, J_{HH} = 4.7 Hz, 1H, H^6); 8.34 (d, J_{HH} = 8 Hz, 1H, H^3); 8.05 (t, J_{HH} = 8 Hz, 1H, H^4); 7.82 (d, J_{HH} = 7.2 Hz, 1H, H$^{3'}$); 7.76 (d, J_{HH} = 7.7 Hz, 1H, H$^{6'}$); 7.57 (m, 1H, H^5); 7.40 (t, J_{HH} = 7.7 Hz, 1H, H$^{5'}$); 7.35 (t, J_{HH} = 7.7 Hz, 1H, H$^{4'}$); 4.97 (t, J_{HH} = 7.2 Hz, 2H, H$^{\gamma}$); 2.43 (t, J_{HH} = 7.8 Hz, 2H, H$^{\alpha}$); 2.13 (m, 2H, H$^{\beta}$) ppm. ^{1}H NMR (D_2O, 298 K): 8.61 (bs, 1H); 7.95 (t, J_{HH} = 7.8 Hz, 1H); 7.84 (d, J_{HH} = 7.4 Hz, 1H); 7.66 (d, J_{HH} = 7.8 Hz, 1H); 7.60 (d, J_{HH} = 7.8 Hz, 1H); 7.49 (t, J_{HH} = 6 Hz, 1H); 7.35 (t, J_{HH} = 7.4 Hz, 1H); 7.29 (t, J_{HH} = 7.8 Hz, 1H); 4.57 (t, J_{HH} = 7.2 Hz, 2H); 2.58 (m, J_{HH} = 7.2 Hz, 2H); 2.02 (q, J_{HH} = 7.2 Hz, 2H) ppm. ^{13}C{^{1}H} NMR (DMSO-d_6, 298 K): 149.2(C^6); 137.6(C^4); 124.8(C^5); 125.7(C^3); 123.8(C$^{5'}$); 123.2(C$^{4'}$); 118.5(C$^{6'}$); 111,7-(C$^{3'}$); 48.4(C$^{\alpha}$); 44.4(C$^{\gamma}$); 26.3(C$^{\beta}$) ppm. Elemental analysis (%): Calculated ($C_{15}H_{14}Cl_2KN_3O_3S{\cdot}H_2O$): C, 48.32; H, 4.32; N, 11.25; S, 8.59. Found: C, 48.43; H, 4.38; N, 10.86; S, 8.69%. IR (ATR): ν(S=O) 1184, 1041 cm^{-1}.

4,4′-bis(N-(4-pentyldiethylamine)carbamoyl)-2,2′-bipyridine (bpyam). Ligand bpyam was synthesized in several steps in nitrogen atmosphere. $SOCl_2$ (3 mL) was added to 200.0 mg (0.8 mmol) of the starting dicarboxylic bipyridine under inert atmosphere, and the mixture was refluxed overnight. The initial white suspension changed to bright yellow solution during the reaction. Solvent was removed under vacuum, and the resulting solid was used without further purification for the following step. 2-Amine-5-diethylaminopentane (320.0 μL, 1.6 mmol) and 230.0 μL (1.6 mmol) of trimethylamine were dissolved in 10 mL of dry dichloromethane, and on this solution another of the acylchloride derivative in 10 mL of dry CH_2Cl_2 was added drop by drop from a pressure equalizing dropping funnel. After it was stirred overnight at room temperature, the solvent was evaporated, obtaining a pink solid, which was washed with diethyl ether four times (4 × 10 mL). In this operation, the remaining chloride acid is removed from the solid mixture. This mixture contains a big amount of $NHEt_3Cl$, which can be removed using an aluminum column of 10 cm long and 1 cm^2 section. The mixture was eluted in 2 mL of MeOH and transferred to the column that was previously wetted with CH_2Cl_2. The reaction product elutes with MeOH/CH_2Cl_2 (4/30 mL). The $NHEt_3Cl$ salt is retained in the column. A pinky-white colored solid was obtained after complete evaporation of the solvents. Yield: 93% (401.5 mg). Elemental analysis (%): Calculated ($C_{30}H_{48}N_6O_2$): C, 68.67; H, 9.22; N, 16.02. Found: C, 68.36; H, 9.82; N, 15.76. ^{1}H NMR (DMSO-d_6, 298 K), δ: 8.87 (d, 2H, J = 5.4 Hz, H^6), 8.80 (bd, 2H, J = 7.3 Hz, NH), 8.79 (s, 2H, H^3), 7.89 (dd, 2H, J = 5.2, J = 1.7 Hz, H^5), 4.10 (m, 2H, H$^{4'}$), 2.42 (q, 8H, J = 7.4 Hz, H$^{6'}$), 2,35 (t, 4H, J = 7.3 Hz, H$^{1'}$), 1.50−1.56 (m, 4H, H$^{3'}$), 1.40−1.44 (m, 4H, H$^{2'}$), 1.21 (d, 6H, J = 6.9 Hz, H$^{5'}$), 1.18 (t, 12H, J = 8.8 Hz, H$^{7'}$) ppm. ^{13}C {^{1}H} NMR (DMSO-d_6, 298 K): 164.21 (CO), 155.49 (C^2), 149.97 (C^6), 143.14 (C^4), 122.11 (C^5), 118.31 (C^3), 50.46 (C$^{1'}$), 46.64 (C$^{6'}$), 44.70 (C$^{4'}$), 32.83 (C$^{3'}$), 20.62 (C$^{2'}$), 20.25 (C$^{5'}$), 8.53

DOI: 10.1021/acs.inorgchem.8b00713
Inorg. Chem. XXXX, XXX, XXX−XXX

($C^{7'}$) ppm. FTIR (ATR): 3429 νNH, 1635 ν(C═O) cm^{-1}. MS-FAB$^+$: 526 (100%, $[M+2H]^+$) m/z.

[$PtCl_2$(pbiCN)], **1**. A solution containing 50 mg of pbiCN (0.2 mmol) in 9 mL of acetone was added to another with 83.6 mg of $K_2[PtCl_4]$ (0.2 mmol) in 4 mL of water. The mixture was stirred at 50 °C for 4 d. The yellow precipitate was filtered and washed with water, ethanol, and diethyl ether (3 mL each one). A yellow solid was obtained. 55.9 mg, yield: 54%. Elemental analysis (%): Calculated ($C_{15}H_{12}Cl_2N_4Pt$): C, 35.03; H, 2.35; N, 10.89. Found: C, 35.51; H, 1.91; N, 10.11. ^{1}H NMR (DMSO-d_6, 298 K): 9.66 (d, J_{HH} = 6.5 Hz, 1H, H^6); 9.01 (d, J_{HH} = 8.3 Hz, 1H, $H^{6'}$); 8.42 (m, 2H, H^3 and H^4); 8.09 (d, J_{HH} = 8.3 Hz, 1H, $H^{3'}$); 7.84 (t, J_{HH} = 6.5 Hz, 1H, H^5); 7.60 (t, J_{HH} = 7.8 Hz, 1H, $H^{4'}$); 7.50 (t, J_{HH} = 7.8 Hz, 1H, $H^{5'}$); 5.20 (t, J_{HH} = 6.4 Hz, 2H, H^{β}); 3.24 (t, J_{HH} = 6.4 Hz, 2H, H^{α}) ppm. The corresponding $^{13}C\{^1H\}$ NMR was not registered, because the complex evolves in DMSO solution. MS-FAB$^+$: 557 (M−Cl+DMSO) m/z. IR (ATR): ν(CN) 2249 cm^{-1}.

[$PtCl_2$(pbiSO$_3$)], **2**. Over a solution containing 76.21 mg of pbiSO$_3$ (0.24 mmol) in 5 mL of acetone, another of $K_2[PtCl_4]$ (100 mg, 0.24 mmol) in 5 mL of water was added. The mixture was stirred at 50 °C for 24 h. The solvent was removed by vacuum evaporation, leaving a brown solid. 111 mg, yield: 74%. Elemental analysis (%): Calculated ($C_{15}H_{14}Cl_2KN_3O_3PtS$): C, 28.29; H, 2.27; N, 6.76; S, 5.26. Found: C, 28.21; H, 2.16; N, 6.82; S, 5.23. ^{1}H NMR (DMSO-d_6, 298 K): 9.63 (d, J = 6.1 Hz, 1H, H^6); 8.95 (d, J = 8.2 Hz, 1H, $H^{6'}$); 8.70 (d, J = 7.9 Hz, 1H, H^3); 8.32 (t, J = 7.9 Hz, 1H, H^4); 8.03 (d, J = 8.2 Hz, 1H, $H^{3'}$); 7.79 (t, J = 6.1 Hz, 1H, H^5); 7.53 (t, J = 7.6 Hz, 1H, $H^{4'}$); 7.43 (t, J = 7.6 Hz, 1H, $H^{5'}$); 4.97 (t, J = 7.9 Hz, 2H, H^{γ}); 2.67 (t, J = 6.2 Hz, 2H, H^{α}); 2.13 (m, 2H, H^{β}) ppm. $^{13}C\{^1H\}$ NMR (DMSO-d_6, 298 K): 150.54 (C^6); 141.18 (C^4); 128.07 (C^5); 126.16 ($C^{4'}$); 125.98 (C^3); 125.74($C^{5'}$); 119.07 ($C^{6'}$); 112.81 ($C^{3'}$); 47.99 (C^{α}); 44.80 (C^{γ}); 25.87 (C^{β}) ppm. MS-FAB$^-$: 582 $[M-K]^-$ m/z. IR (ATR): ν(S═O) 1184, 1043 cm^{-1}.

[$PtCl_2$(bpyam)], **3**. The product was obtained by diffusion of the reactants in phases. In a crystallization tube under inert atmosphere, three phases were added: the lower phase consisted of a $K_2[PtCl_4]$ solution (15.8 mg, 0.04 mmol) in 2 mL of water; middle phase of 1 mL of water; the upper phase consisted of the ligand solution of (20.0 mg, 0.04 mmol) in 1 mL of water. Phases were allowed to fully diffuse. The precipitate was filtered and washed with water, affording the product as a yellow solid. Yield: 56% (17.7 mg). The product can be obtained in a bigger amount by direct reaction in Schlenk, by stirring overnight. Elemental analysis (%): Calculated ($C_{30}H_{48}Cl_2N_6O_2Pt$): C: 45.57, H: 6.12, N: 10.63. Found: C: 45.31, H: 6.25, N: 10.42. ^{1}H NMR (DMSO-d_6, 298 K), δ: 9.63 (d, 2H, J = 5.4, H^6), 9.60 (bs, 2H, $H^3{}_{A\ or\ B}$), 9.46 (bs, 2H, $H^3{}_{A\ or\ B}$), 9.45(bs, 2H, -N*H*Et$_2$), 9.16, (d, 2H, J = 5.3, $NH_{A\ or\ B}$), 9.13 (d, 2H, J = 5.3, $NH_{A\ or\ B}$), 8.23 (m, 2H, H^5), 4.14 (m, 2H, $H^{4'}$), 2.92 (m, 12H, $H^{1'}$ + $H^{6'}$), 1.55−1.80 (m, 8H, $H^{2'}$ + $H^{3'}$), 1.27 (d, 6H, J = 6.3 Hz, $H^{5'}$), 1.13 (bs, 12H, $H^{7'}$) ppm. $^{13}C\{^1H\}$ NMR (DMSO-d_6, 298 K): 161.60 ($CO_{A\ or\ B}$), 161.52 ($CO_{A\ or\ B}$), 157.27 ($C^2{}_{A\ or\ B}$), 157.23 ($C^2{}_{A\ or\ B}$), 148.96 (C^6), 143.77 ($C^4{}_{A\ or\ B}$), 143.65 ($C^4{}_{A\ or\ B}$), 126.12 (C^5), 121.74 ($C^3{}_{A\ or\ B}$), 121.68 ($C^3{}_{A\ or\ B}$), 50.71 ($C^{1'}$), 46.10 ($C^{6'}$), 45.48 ($C^{4'}{}_{A\ or\ B}$), 45.42 ($C^{4'}{}_{A\ or\ B}$), 32.73 ($C^{3'}$), 20.59 ($C^{5'}$), 20.56 ($C^{2'}$), 9.14 ($C^{7'}$) ppm. A and B stands for the two diastereomers (if not indicated, the resonance signal for both diastereomers is the same). Fourier transform infrared attenuated total reflectance (FTIR ATR): 3432 ν(NH), 1637 ν(C═O) cm^{-1}. MS-FAB$^+$: 792 (15%, $[M+2H]^+$); 756 (7%, $[M-Cl+H]^+$); 526 (100%, $[L+2H]^+$) m/z.

[$PtCl_2$(bpyst)], **4**. Ligand of this complex ((4,4′-bis(α-styrene)-2,2′-bipyridine (bpyst)) was prepared as previously reported.[28] A yellow colored solution of $[PtCl_2(NCPh)_2]$ was prepared in 40 mL of dichloroethane (106.7 mg, 0.226 mmol). Over this solution another solution of the ligand bpyst was added (82 mg, 0.226 mmol). The suspension was maintained for 2 d at 60 °C. The formation of a yellow precipitate was observed, and the solution turned to yellow-brown. The precipitate was filtered, and the solution was evaporated to 3 mL. Diethyl ether was added to complete precipitation of a solid. The solution was sonicated for 5 min and filtered out in a porous glass filter. The obtained brown solid was washed with diethyl ether (3 × 3 mL) and dried under vacuum. Yield: 65% (92.3 mg). Elemental analysis (%): Calculated ($C_{26}H_{22}Cl_2N_2Pt$): C: 49.69, H: 3.53, N: 4.46. Found: C: 49.51, H: 3.64, N: 4.37. ^{1}H NMR (DMSO-d_6, 298 K), δ: 9.40 (d, 2H, J_{HH} = 6.2 Hz, H^6); 8.85 (s, 2H, H^3); 7.99 (d, 2H, J_{HH} = 16.5 Hz, H^{olef}), 7.94 (d, 2H, J_{HH} = 6.2 Hz, H^5); 7.77 (d, 4H, J_{HH} = 7.8 Hz, H°); 7.53−7.45 (m, 8H, H^m, H^p, and H^{olef}) ppm. The corresponding $^{13}C\{^1H\}$ NMR resonances are not indicated, because the signals are too broad for a proper assignment. FTIR (ATR): 1612 (ν(C═C) cm^{-1}. MS-FAB$^+$: 591 (4%, M−Cl−2H) m/z.

General Procedure of Stability and Binding to dGMP by NMR Studies. *Stability in DMSO-d_6.* Complexes **1**−**4** (5−8 mg) were dissolved in 0.5 mL of DMSO-d_6, and ^{1}H NMR spectra were recorded during 7 d in a 400 MHz spectrometer.

Aquation Studies. Over the previous solution, 50 μL of D_2O was added, and ^{1}H NMR spectra were recorded during 7 d in a 400 MHz spectrometer.

Binding Studies to dGMP. Over the solution coming from the aquation studies, 5 mg of dGMP dissolved in 20 μL of D_2O was added, and ^{1}H NMR and $^{31}P\{^1H\}$ spectra were recorded during 5 d in a 400 MHz spectrometer.

UV−Vis Spectroscopy. Absorbance measurements were performed to study the substitution of the chloro ligands of the metal complexes for DMSO and H_2O molecules when NMR experiments were not suitable because of precipitation phenomena. Measurements were performed on a Hewlett-Packard 8453A (Agilent Technologies) photodiode array spectrophotometer fitted out with a Peltier temperature control system at T = 25 °C in 1.0 cm path-length cells.

Circular Dichroism. CD studies were performed by incubating ctDNA or BSA with the metal complexes for 72 h, in sodium cacodylate (NaCac) buffer (I = 2.5 mM) at pH = 7.4 and T = 25 °C and recording the CD spectra with a MOS-450 biological spectrophotometer (Bio-Logic SAS) in 1.0 cm path-length cells. As DMSO can affect the CD spectra of the biomolecules, the control measurements (ctDNA or BSA in the absence of metal complex) were incubated with the same DMSO percentage as the samples under the same experimental condition.

Differential Scanning Calorimetry. To prepare the DSC samples, ctDNA (4×10^{-4} M) was incubated with the metal complexes for 72 h, in NaCac buffer (I = 2.5 mM) at pH = 7.4 and T = 25 °C. For the control measurement, ctDNA in the absence of metal complex was incubated with the same DMSO content as the other samples under the same experimental conditions. Before recording the DSC measurements, the samples were degassed for 30 min in a degassing station (TA Instruments). DSC thermal denaturation studies were performed with a nano DSC (TA Instruments) by scanning at 3 atm pressure from 25 to 95 °C at 1 °C·min^{-1} scan rate. The DCS curves were analyzed using the NanoAnalyze (TA Instruments) software.

Viscosity Measurements. Viscosity measurements were performed with an Ubbelohde viscometer (Schott) immersed in a water bath at T = 25 °C. The flow time was measured with a digital stopwatch. The sample viscosity was evaluated as the mean value of at least four replicated measurements. The viscosity readings were reported as $L/L_0 = (\eta/\eta_0)^{1/3}$ versus C_D/C_P ratio, where η and η_0 stand for the polynucleotide viscosity in the presence and in the absence of the metal complex, respectively.

Cytotoxic Activity. 2.5×10^3 HeLa (human cervical carcinoma) or A549 (human lung carcinoma) cells were seeded in 200 μL culture medium per well (DMEM medium), supplemented with 10% FBS and 1% amphotericin-penicillin-streptomycin solution in 96-well plates and incubated in a humid atmosphere at 37 °C under 5% CO_2 atmosphere for 24 h. Cells were then incubated for 72 h with 100 μL of culture medium (supplemented either with 10% or 1% of FBS) with different concentrations of the metal complexes in culture medium. Cisplatin was also included as a positive control. Then, 100 μL of 500 μg/mL of MTT (thiazolyl blue tetrazolium bromide) was added to each well and incubated for 4 h. Lastly, the formazan product was dissolved by adding 100 μL of solubilizing solution (10% sodium dodecyl sulfate (SDS) in 0.01 M HCl) and allowing the solution to solubilize overnight. Absorbance was read at 590 nm in a microplate reader

DOI: 10.1021/acs.inorgchem.8b00713
Inorg. Chem. XXXX, XXX, XXX−XXX

(Biotek Instruments). Four replicates per dose were included in each experiment, and half-maximal inhibitory concentration (IC_{50}) values were calculated using the GraphPad Prism 6.01 analysis software (GraphPad Software Inc.) from three independent experiments.

Native Protein Electrophoresis. Native polyacrylamide gel electrophoresis (PAGE) was performed by incubating BSA overnight with different concentrations of the platinum complexes for [complex]/[protein] concentration ratios of 10 and 20 in Tris HCl buffer (0.5 M, pH = 6.8) and T = 25 °C. After that, 5 μL of sample buffer 2X (0.01% bromophenol blue and 20% glycerol in Tris HCl buffer (0.5 M, pH 6.8) were added to 5 μL of the sample solutions and loaded onto 10% polyacrylamide gels. Gels were run in tris borate and EDTA (TBE) ×1 buffer at 80 V for 4 h at 4 °C to avoid denaturation of the protein. Finally, gels were stained with Coomassie Brilliant Blue R-250 and visualized with a Gel Doc XR+ Imaging System (Bio-Rad).

Agarose Gel Electrophoresis. Agarose gel electrophoresis of plasmid DNA (pUC18) was performed after incubation of the plasmid (15 μM, base pairs) in the presence of different concentrations of complex **4** (1.5−750 μM) or cisplatin (15 and 150 μM) for 72 h. A vehicle-treated pUC18 sample was included with the maximum DMSO concentration used in the electrophoresis experiment. Loading buffer (2 μL) was added to each sample (10 μL) prior to being loaded onto a 1% agarose gel containing 0.05 μg mL^{-1} ethidium bromide. Electrophoresis was run at 5 V/cm for 2 h in TBE ×1 buffer, and the gel was visualized with a Gel Doc XR+ Imaging System (Bio-Rad).

Cellular Uptake Studies. A549 cells were seeded in culture flasks (2.5×10^6 cells in 6 mL DMEM culture medium and incubated for 24 h at 37 °C and 5% CO_2. After that, cells were treated with the indicated concentrations of the Pt complexes for 24 h and harvested in phosphate buffered saline. The samples were digested with 65% HNO_3 at room temperature for 24 h and then diluted with Milli-Q water to obtain 2% HNO_3 solutions to be analyzed by inductively coupled plasma-mass spectrometry (ICP-MS).

Computational Details. The geometries of reactants, intermediates, products, and transition states were fully optimized by DFT calculations, using the B3LYP,[49] PBE0,[50] and M06-2X[51] functionals, the CEP-121G[52] effective potential basis set for the Pt atom, and the 6-31G(d,p)[53] basis set for the other atoms, as recently reported.[54,55] Water solvent effects were mimicked by the "conductor-like polarized continuum model" implicit method.[56] The reaction pathway leading to hydrolysis of **4** was followed by a two-step nucleophilic substitution mechanism, widely accepted and reported in the literature.[57] The geometry of the transition states was optimized by the synchronous transit quasi-Newton method.[58] Vibrational analysis, in the harmonic approximation, was performed. This allowed us to evaluate also the enthalpy and the Gibbs free energy differences along the reaction pathways. Energy minimum structures presented no imaginary frequencies, while all transition states were first-order saddle points in the potential energy surface. All calculations were performed with the Guassian09 package.[59]

■ ASSOCIATED CONTENT

Supporting Information

The Supporting Information is available free of charge on the ACS Publications website at DOI: 10.1021/acs.inorgchem.8b00713.

Experimental details including the stability in DMSO and aqueous buffer of compound **1**, NMR spectra for compounds **2** and **3** in the presence of dGMP and for compound **4**: relative energy obtained by DFT calculations, agarose gel electrophoresis of plasmid pUC18, CD spectra, and relative elongation of ctDNA in the presence of different concentrations of complex (PDF)

■ AUTHOR INFORMATION

Corresponding Author

*E-mail: begar@ubu.es.

ORCID

Natalia Busto: 0000-0001-9637-1209
Giampaolo Barone: 0000-0001-8773-2359
Mónica Vaquero: 0000-0002-4550-4072
Félix A. Jalón: 0000-0002-6622-044X
Blanca R. Manzano: 0000-0002-4908-4503
Begoña García: 0000-0002-0817-1651

Notes

The authors declare no competing financial interest.

■ ACKNOWLEDGMENTS

The authors gratefully acknowledge the financial support by La Caixa Foundation (LCF/PR/PR12/11070003), Ministerio de Economía y Competitividad-FEDER (CTQ2014-58812-C2-2-R, CTQ2014-58812-C2-1-R, and CTQ2015-70371-REDT), Consejería de Educación−Junta de Castilla y León-FEDER (BU042U16), Spain. C.P.-A. is grateful for the FPU grant from Ministry of Education, Culture and Sports, Madrid, Spain (FPU13/00180).

■ REFERENCES

(1) Galluzzi, L.; Senovilla, L.; Vitale, I.; Michels, J.; Martins, I.; Kepp, O.; Castedo, M.; Kroemer, G. Molecular Mechanisms of Cisplatin Resistance. *Oncogene* **2012**, *31*, 1869−1883.

(2) Florea, A.-M.; Buesselberg, D. Cisplatin as an Anti-Tumor Drug: Cellular Mechanisms of Activity, Drug Resistance and Induced Side Effects. *Cancers* **2011**, *3*, 1351−1371.

(3) Shekar, K.; Mcdonald, C. I.; Mullany, D. V.; Fraser, J. F.; Roberts, J. A.; Wallis, S. C.; Ghassabian, S.; Anstey, C.; Fung, Y. L. Protein-Bound Drugs Are Prone to Sequestration in the Extracorporeal Membrane Oxygenation Circuit: Results from an Ex Vivo Study. *Crit. Care* **2015**, *19*, 164.

(4) Haghdoost, M. M.; Golbaghi, G.; Létourneau, M.; Patten, S. A.; Castonguay, A. Lipophilicity-Antiproliferative Activity Relationship Study Leads to the Preparation of a ruthenium(II) Arene Complex with Considerable in Vitro Cytotoxicity against Cancer Cells and a Lower in Vivo Toxicity in Zebrafish Embryos than Clinically Approved c. *Eur. J. Med. Chem.* **2017**, *132*, 282−293.

(5) Babak, M. V.; Pfaffeneder-Kmen, M.; Meier-Menches, S. M.; Legina, M. S.; Theiner, S.; Licona, C.; Orvain, C.; Hejl, M.; Hanif, M.; Jakupec, M. A.; Keppler, B. K.; Gaiddon, C.; Hartinger, C. G. Rollover Cyclometalated Bipyridine Platinum Complexes as Potent Anticancer Agents: Impact of the Ancillary Ligands on the Mode of Action. *Inorg. Chem.* **2018**, *57*, 2851−2864.

(6) Gabano, E.; Gama, S.; Mendes, F.; Fregonese, F.; Paulo, A.; Ravera, M. Application of Microwave-Assisted Heating to the Synthesis of Pt(II) Complexes. *Inorg. Chim. Acta* **2015**, *437*, 16−19.

(7) Mock, C.; Puscasu, I.; Rauterkus, M. J.; Tallen, G.; Wolff, J. E. A.; Krebs, B. Novel Pt(II) Anticancer Agents and Their Pd(II) Analogues: Syntheses, Crystal Structures, Reactions with Nucleobases and Cytotoxicities. *Inorg. Chim. Acta* **2001**, *319*, 109−116.

(8) Casas, J. S.; Castiñeiras, A.; García-Martínez, E.; Parajó, Y.; Pérez-Parallé, M. L.; Sánchez-González, A.; Sordo, J. Synthesis and Cytotoxicity of 2-(2′-Pyridyl)benzimidazole Complexes of palladium-(II) and platinum(II). *Z. Anorg. Allg. Chem.* **2005**, *631*, 2258−2264.

(9) Serratrice, M.; Maiore, L.; Zucca, A.; Stoccoro, S.; Landini, I.; Mini, E.; Massai, L.; Ferraro, G.; Merlino, A.; Messori, L.; Cinellu, M. A. Cytotoxic Properties of a New Organometallic platinum(II) Complex and Its gold(I) Heterobimetallic Derivatives. *Dalton Trans.* **2016**, *45*, 579−590.

(10) Labadie, S.; Dragovich, P. S.; Barrett, K.; Blair, W. S.; Bergeron, P.; Chang, C.; Deshmukh, G.; Eigenbrot, C.; Ghilardi, N.; Gibbons, P.;

DOI: 10.1021/acs.inorgchem.8b00713
Inorg. Chem. XXXX, XXX, XXX−XXX

Hurley, C. A.; Johnson, A.; Kenny, J. R.; Kohli, P. B.; Kulagowski, J. J.; Liimatta, M.; Lupardus, P. J.; Mendonca, R.; Murray, J. M.; Pulk, R.; Shia, S.; Steffek, M.; Ubhayakar, S.; Ultsch, M.; van Abbema, A.; Ward, S.; Zak, M. Structure-Based Discovery of C-2 Substituted Imidazo-Pyrrolopyridine JAK1 Inhibitors with Improved Selectivity over JAK2. *Bioorg. Med. Chem. Lett.* **2012**, *22*, 7627−7633.

(11) Fernandez, G. A.; Vela Gurovic, M. S.; Olivera, N. L.; Chopa, A. B.; Silbestri, G. F. Antibacterial Properties of Water-Soluble gold(I) N-Heterocyclic Carbene Complexes. *J. Inorg. Biochem.* **2014**, *135*, 54−57.

(12) Marinelli, M.; Pellei, M.; Cimarelli, C.; Dias, H. V. R.; Marzano, C.; Tisato, F.; Porchia, M.; Gandin, V.; Santini, C. Novel Multicharged silver(I)-NHC Complexes Derived from Zwitterionic 1,3-Symmetrically and 1,3-Unsymmetrically Substituted Imidazoles and Benzimidazoles: Synthesis and Cytotoxic Properties. *J. Organomet. Chem.* **2016**, *806*, 45−53.

(13) Smith, K. A.; Conboy, J. C. Using Micropatterned Lipid Bilayer Arrays to Measure the Effect of Membrane Composition on Merocyanine 540 Binding. *Biochim. Biophys. Acta, Biomembr.* **2011**, *1808*, 1611−1617.

(14) Schlegel, R. A.; Phelps, B. M.; Waggoner, A.; Terada, L.; Williamson, P. Binding of Merocyanine 540 to Normal and Leukemic Erythroid Cells. *Cell* **1980**, *20*, 321−328.

(15) Ecker, A.; Lehane, A. M.; Clain, J.; Fidock, D. A. PfCRT and Its Role in Antimalarial Drug Resistance. *Trends Parasitol.* **2012**, *28*, 504−514.

(16) Rahim, R.; Strobl, J. S. Hydroxychloroquine, Chloroquine, and All-Trans Retinoic Acid Regulate Growth, Survival, and Histone Acetylation in Breast Cancer Cells. *Anti-Cancer Drugs* **2009**, *20*, 736−745.

(17) Das, S.; Preet, R.; Siddharth, S.; Nayak, A.; Kundu, C. N.; Tripathi, N.; Bharatam, P. V. Quinacrine Induces Apoptosis in Cancer Cells by Forming a Functional Bridge between TRAIL-DR5 Complex and Modulating the Mitochondrial Intrinsic Cascade. *Oncotarget* **2017**, *8*, 248−267.

(18) Zhu, J.; Zheng, Y.; Zhang, H.; Zhu, J.; Sun, H.; Zhu, J.; Zheng, Y.; Zhang, H.; Zhu, J. Low Concentration of Chloroquine Enhanced Efficacy of Cisplatin in the Treatment of Human Ovarian Cancer Dependent on Autophagy. *Am. J. Transl. Res.* **2017**, *9*, 4046−4058.

(19) Wang, Y.; Bi, Q.; Dong, L.; Li, X.; Ge, X.; Zhang, X.; Fu, J.; Wu, D.; Li, S. Quinacrine Enhances Cisplatin-Induced Cytotoxicity in Four Cancer Cell Lines. *Chemotherapy* **2010**, *56*, 127−134.

(20) Dreyse, P.; Gonzalez, I.; Cortes-Arriagada, D.; Ramirez, O.; Salas, I.; Gonzalez, A.; Toro-Labbe, A.; Loeb, B. New Cyclometalated Ir(III) Complexes with Bulky Ligands with Potential Applications in LEC Devices: Experimental and Theoretical Studies of Their Photophysical Properties. *New J. Chem.* **2016**, *40*, 6253−6263.

(21) Gajardo, F.; Barrera, M.; Vargas, R.; Crivelli, I.; Loeb, B. Influence of the Nature of the Absorption Band on the Potential Performance of High Molar Extinction Coefficient Ruthenium(II) Polypyridinic Complexes As Dyes for Sensitized Solar Cells. *Inorg. Chem.* **2011**, *50*, 5910−5924.

(22) Dreyse, P.; Loeb, B.; Soto-Arriaza, M.; Tordera, D.; Orti, E.; Serrano-Perez, J. J.; Bolink, H. J. Effect of Free Rotation in Polypyridinic Ligands of Ru(II) Complexes Applied in Light-Emitting Electrochemical Cells. *Dalton Trans.* **2013**, *42*, 15502−15513.

(23) Maury, O.; Guegan, J.-P.; Renouard, T.; Hilton, A.; Dupau, P.; Sandon, N.; Toupet, L.; Le Bozec, H. Design and Synthesis of 4,4′-π-conjugated[2,2′]-Bipyridines: A Versatile Class of Tunable Chromophores and Fluorophores. *New J. Chem.* **2001**, *25*, 1553−1566.

(24) Baccouche, A.; Peigne, B.; Ibersiene, F.; Hammoutene, D.; Boutarfaia, A.; Boucekkine, A.; Feuvrie, C.; Maury, O.; Ledoux, I.; Le Bozec, H. Effects of the Metal Center and Substituting Groups on the Linear and Nonlinear Optical Properties of Substituted Styryl-Bipyridine Metal(II) Dichloride Complexes: DFT and TDDFT Computational Investigations and Harmonic Light Scattering Measurements. *J. Phys. Chem. A* **2010**, *114*, 5429−5438.

(25) Hossain, M. D.; Haga, M.-A.; Gholamkhass, B.; Nozaki, K.; Tsushima, M.; Ikeda, N.; Ohno, T. Syntheses, Spectroelectrochemistry and Photoinduced Electron-Transfer Processes of Novel Ru and Os Dyad and Triad Complexes with Functionalized Diimide Ligands. *Collect. Czech. Chem. Commun.* **2001**, *66*, 307−337.

(26) Po, C.; Tam, A. Y.-Y.; Wong, K. M.-C.; Yam, V. W.-W. Supramolecular Self-Assembly of Amphiphilic Anionic Platinum(II) Complexes: A Correlation between Spectroscopic and Morphological Properties. *J. Am. Chem. Soc.* **2011**, *133*, 12136−12143.

(27) N'Dongo, H. W. P.; Neundorf, I.; Merz, K.; Schatzschneider, U. Synthesis, Characterization, X-Ray Crystallography, and Cytotoxicity of a Cymantrene Keto Carboxylic Acid for IR Labelling of Bioactive Peptides on a Solid Support. *J. Inorg. Biochem.* **2008**, *102*, 2114−2119.

(28) Kuang, D.; Klein, C.; Ito, S.; Moser, J.-E.; Humphry-Baker, R.; Evans, N.; Duriaux, F.; Gratzel, C.; Zakeeruddin, S. M.; Gratzel, M. High-Efficiency and Stable Mesoscopic Dye-Sensitized Solar Cells Based on a High Molar Extinction Coefficient Ruthenium Sensitizer and Nonvolatile Electrolyte. *Adv. Mater.* **2007**, *19*, 1133−1137.

(29) Andrews, S. S.; Boxer, S. G. Vibrational Stark Effects of Nitriles I. Methods and Experimental Results. *J. Phys. Chem. A* **2000**, *104*, 11853−11863.

(30) Czegeni, C. E.; Papp, G.; Katho, A.; Joo, F. Water-Soluble gold(I)-NHC Complexes of Sulfonated IMes and SIMes and Their Catalytic Activity in Hydration of Alkynes. *J. Mol. Catal. A: Chem.* **2011**, *340*, 1−8.

(31) Condirston, D. A.; Laposa, J. D. Vibrational Spectra of Styrene-H8, -D3, -D5, and -D8. *J. Mol. Spectrosc.* **1976**, *63*, 466−477.

(32) Kelland, L. R. Preclinical Perspectives on Platinum Resistance. *Drugs* **2000**, *59*, 1−8.

(33) Michalke, B. Platinum Speciation Used for Elucidating Activation or Inhibition of Pt-Containing Anti-Cancer Drugs. *J. Trace Elem. Med. Biol.* **2010**, *24*, 69−77.

(34) Busto, N.; Valladolid, J.; Martinez-Alonso, M.; Lozano, H. J.; Jalon, F. A.; Manzano, B. R.; Rodriguez, A. M.; Carrion, M. C.; Biver, T.; Leal, J. M.; Espino, G.; García, B. Anticancer Activity and DNA Binding of a Bifunctional Ru(II) Arene Aqua-Complex with the 2,4-Diamino-6-(2-Pyridyl)-1,3,5-Triazine Ligand. *Inorg. Chem.* **2013**, *52*, 9962−9974.

(35) Macquet, J. P.; Butour, J. L. A Circular Dichroism Study of DNA.platinum Complexes. Differentiation between Monofunctional, Cis-Bidentate and Trans-Bidentate Platinum Fixation on a Series of DNAs. *Eur. J. Biochem.* **1978**, *83*, 375−387.

(36) Fridman, A. S.; Galyuk, E. N.; Vorob'ev, V. I.; Skvortsov, A. N.; Lando, D. Y. Melting of Crosslinked DNA: VI. Comparison of Influence of Interstrand Crosslinks and Other Chemical Modifications Formed by Antitumor Compounds on DNA Stability. *J. Biomol. Struct. Dyn.* **2008**, *26*, 175−185.

(37) Sullivan, M. P.; Holtkamp, H. U.; Hartinger, C. G. Antitumor Metallodrugs That Target Proteins. *Met. Ions Life Sci.* **2018**, *18*, 351−386.

(38) Rubbiani, R.; Can, S.; Kitanovic, I.; Alborzinia, H.; Stefanopoulou, M.; Kokoschka, M.; Mönchgesang, S.; Sheldrick, W. S.; Wölfl, S.; Ott, I. Comparative in Vitro Evaluation of N-Heterocyclic Carbene gold(I) Complexes of the Benzimidazolylidene Type. *J. Med. Chem.* **2011**, *54*, 8646−8657.

(39) Neault, J. F.; Tajmir-Riahi, H. A. Interaction of Cisplatin with Human Serum Albumin. Drug Binding Mode and Protein Secondary Structure. *Biochim. Biophys. Acta, Protein Struct. Mol. Enzymol.* **1998**, *1384*, 153−159.

(40) Pracharova, J.; Vigueras, G.; Novohradsky, V.; Cutillas, N.; Janiak, C.; Kostrhunova, H.; Kasparkova, J.; Ruiz, J.; Brabec, V. Exploring the Effect of Polypyridyl Ligands on the Anticancer Activity of Phosphorescent Iridium(III) Complexes: From Proteosynthesis Inhibitors to Photodynamic Therapy Agents. *Chem. - Eur. J.* **2018**, *24*, 1−14.

(41) Kragh-Hansen, U. Molecular Aspects of Ligand Binding to Serum Albumin. *Pharmacol. Rev.* **1981**, *33* (1), 17−53.

(42) Markovic, O. S.; Cvijetic, I. N.; Zlatovic, M. V.; Opsenica, I. M.; Konstantinovic, J. M.; Terzic Jovanovic, N. V.; Solaja, B. A.; Verbic, T. Z. Human Serum Albumin Binding of Certain Antimalarials. *Spectrochim. Acta, Part A* **2018**, *192*, 128−139.

DOI: 10.1021/acs.inorgchem.8b00713
Inorg. Chem. XXXX, XXX, XXX−XXX

(43) Schroeder, R. L.; Pendleton, P.; Gerber, J. P. Physical Factors Affecting Chloroquine Binding to Melanin. *Colloids Surf., B* **2015**, *134*, 8−16.
(44) Valko, K.; Nunhuck, S.; Bevan, C.; Abraham, M. H.; Reynolds, D. P. Fast Gradient HPLC Method to Determine Compounds Binding to Human Serum Albumin. Relationships with Octanol/water and Immobilized Artificial Membrane Lipophilicity. *J. Pharm. Sci.* **2003**, *92*, 2236−2248.
(45) Fulmer, G. R.; Miller, A. J. M.; Sherden, N. H.; Gottlieb, H. E.; Nudelman, A.; Stoltz, B. M.; Bercaw, J. E.; Goldberg, K. I. NMR Chemical Shifts of Trace Impurities: Common Laboratory Solvents, Organics, and Gases in Deuterated Solvents Relevant to the Organometallic Chemist. *Organometallics* **2010**, *29*, 2176−2179.
(46) Boutain, M.; Duckett, S. B.; Dunne, J. P.; Godard, C.; Hernandez, J. M.; Holmes, A. J.; Khazal, I. G.; Lopez-Serrano, J. A Parahydrogen Based NMR Study of Pt Catalysed Alkyne Hydrogenation. *Dalton Trans.* **2010**, *39*, 3495−3500.
(47) Felsenfeld, G.; Hirschman, S. Z. A Neighbor-Interaction Analysis of the Hypochromism and Spectra of DNA. *J. Mol. Biol.* **1965**, *13*, 407−427.
(48) Azzazy, H. M. E.; Christenson, R. H. *All about Albumin: Biochemistry, Genetics, and Medical Applications;* Academic Press, 1996.
(49) Devlin, F. J.; Finley, J. W.; Stephens, P. J.; Frisch, M. J. Ab Initio Calculation of Vibrational Absorption and Circular Dichroism Spectra Using Density Functional Force Fields: A Comparison of Local, Nonlocal, and Hybrid Density Functionals. *J. Phys. Chem.* **1995**, *99*, 16883−16902.
(50) Adamo, C.; Barone, V. Toward Reliable Density Functional Methods without Adjustable Parameters: The PBE0Model. *J. Chem. Phys.* **1999**, *110*, 6158−6170.
(51) Zhao, Y.; Truhlar, D. G. The M06 Suite of Density Functionals for Main Group Thermochemistry, Thermochemical Kinetics, Noncovalent Interactions, Excited States, and Transition Elements: Two New Functionals and Systematic Testing of Four M06-Class Functionals and 12 Other Function. *Theor. Chem. Acc.* **2008**, *120*, 215−241.
(52) Stevens, W. J.; Krauss, M.; Basch, H.; Jasien, P. G. Relativistic Compact Effective Potentials and Efficient, Shared-Exponent Basis Sets for the Third-, Fourth-, and Fifth-Row Atoms. *Can. J. Chem.* **1992**, *70*, 612−630.
(53) Petersson, G. A.; Bennett, A.; Tensfeldt, T. G.; Al-Laham, M. A.; Shirley, W. A.; Mantzaris, J. A Complete Basis Set Model Chemistry. I. The Total Energies of Closed-Shell Atoms and Hydrides of the First-Row Elements. *J. Chem. Phys.* **1988**, *89*, 2193−2218.
(54) Lauria, A.; Almerico, A. M.; Barone, G. The Influence of Substitution in the Quinoxaline Nucleus on 1,3-Dipolar Cycloaddition Reactions: A DFT Study. *Comput. Theor. Chem.* **2013**, *1013*, 116−122.
(55) Bonsignore, R.; Russo, F.; Terenzi, A.; Spinello, A.; Lauria, A.; Gennaro, G.; Almerico, A. M.; Keppler, B. K.; Barone, G. The Interaction of Schiff Base Complexes of nickel(II) and zinc(II) with Duplex and G-Quadruplex DNA. *J. Inorg. Biochem.* **2018**, *178*, 106−114.
(56) Cossi, M.; Rega, N.; Scalmani, G.; Barone, V. Energies, Structures, and Electronic Properties of Molecules in Solution with the C-PCM Solvation Model. *J. Comput. Chem.* **2003**, *24*, 669−681.
(57) Lau, J. K.-C.; Ensing, B. Hydrolysis of Cisplatin—a First-Principles Metadynamics Study. *Phys. Chem. Chem. Phys.* **2010**, *12* (35), 10348−10355.
(58) Peng, C.; Ayala, P.; Schlegel, H. B.; Frisch, M. J. Using Redundant Internal Coordinates to Optimize Equilibrium Geometries and Transition States. *J. Comput. Chem.* **1996**, *17*, 49−56.
(59) Frisch, M. J.; Trucks, G. W.; Schlegel, H. B.; Scuseria, G. E.; Robb, M. A.; Cheeseman, J. R.; Scalmani, G.; Barone, V.; Petersson, G. A.; Nakatsuji, H.; Li, X.; Caricato, M.; Marenich, A.; Bloino, J.; Janesko, B. G.; Gomperts, R.; Menucci, B.; Hratchian, H. P.; Ortiz, J. V.; Izmaylov, A. F.; Sonnenberg, J. L.; Williams-Young, D., Ding, F.; Lipparini, F.; Egidi, F.; Goings, J.; Peng, B.; Petrone, A.; Henderson, T.; Ranasinghe, D.; Zakrzewski, V. G.; Gao, J.; Rega, N.; Zheng, G.; Liang, W.; Hada, M.; Ehara, M.; Toyota, K.; Fukuda, R.; Hasegawa, J.; Ishida, M.; Nakijama, T.; Honda, Y.; Kitao, O.; Nakai, H.; Vreven, T.; Throssell, K.; Montgomery, J. A., Jr; Peralta, J. E.; Ogliaro, F.; Bearpark, M.; Heyd, J. J.; Brothers, E.; Kudin, K. N.; Staroverov, V. N.; Keith, T.; Kobayasi, R.; Normand, J.; Raghavachari, K.; Rendell, A.; Burant, J. C.; Iyengar, S. S.; Tomasi, J.; Cossi, M.; Millam, J. M.; Klene, M.; Adamo, C.; Cammi, R.; Ochterski, J. W.; Martin, L. R.; Morokuma, K.; Farkas, O.; Foresman, J. B.; Fox, D. J. *Gaussian 09;* Gaussian, Inc.: Wallingford, CT, 2016.

DOI: 10.1021/acs.inorgchem.8b00713
Inorg. Chem. XXXX, XXX, XXX−XXX